

Citation for published version:
Sun, Y, Yu, F₃Liao, M, Ma, J, Wang, X, He, D, Gao, W, Knight, J & Hu, L 2020, 'Visible emission and energy transfer in Tb /Dy co-doped phosphate glasses', *Journal of the American Ceramic Society*, vol. 103, no. 12, pp. 6847-6859. https://doi.org/10.1111/jace.17391

10.1111/jace.17391

Publication date: 2020

Document Version Peer reviewed version

Link to publication

This is the peer reviewed version of the following article: Sun, Y, Yu, F, Liao, M, et al. Visible emission and energy transfer in Tb3+/Dy3+ codoped phosphate glasses. J Am Ceram Soc. 2020; 00: 1– 13., which has been published in final form at https://doi.org/10.1111/jace.17391. This article may be used for non-commercial purposes in accordance with Wiley Terms and Conditions for Self-Archiving.

University of Bath

Alternative formats

If you require this document in an alternative format, please contact: openaccess@bath.ac.uk

Copyright and moral rights for the publications made accessible in the public portal are retained by the authors and/or other copyright owners and it is a condition of accessing publications that users recognise and abide by the legal requirements associated with these rights.

Take down policyIf you believe that this document breaches copyright please contact us providing details, and we will remove access to the work immediately and investigate your claim.

Download date: 07 Mar 2023

Visible emission and energy transfer in Tb³⁺/Dy³⁺ co-doped phosphate glasses

Yan Sun ^{1,2}, Fei Yu ^{1,3}*, Meisong Liao ¹, Juping Ma ^{1,2}, Xin Wang ¹, Dongbing He ¹, Weiqing Gao ⁴,

Jonathan Knight ⁵, Lili Hu ^{1,3,*}

¹ Key Laboratory of Materials for High Power Laser, Shanghai Institute of Optics and Fine Mechanics,

Chinese Academy of Sciences, Shanghai 201800, China

² Center of Materials Science and Optoelectronics Engineering, University of Chinese Academy of

Sciences, Beijing 100049, China

³ Hangzhou Institute for Advanced Study, University of Chinese Academy of Sciences, Hangzhou 310024,

China

⁴ Department of Optical Engineering, Hefei University of Technology, Hefei 230601, China

⁵ Centre for Photonics and Photonic Materials, Department of Physics, University of Bath, Claverton

Down, Bath, BA2 7AY, United Kingdom

Abstract: In this work, we systematically study spectroscopic properties of Tb³⁺/Dy³⁺ co-doped phosphate

glasses in the visible spectral region and explore the sensitization role of Dy³⁺ in the enhancement of visible

fluorescence of Tb³⁺ ions. Judd–Ofelt parameters Ω_2 and Ω_4/Ω_6 of the phosphate glass as host for Tb³⁺ are

calculated as 21.60×10^{-20} cm² and 0.73 respectively based on the measured spectral absorption. Multiple

energy transfer routes from Dy3+ to Tb3+ and their efficiencies are characterized and the enhanced

fluorescence properties of Tb3+ are investigated, including the emission spectral strength and the

spontaneous emission lifetime as functions of Dy³⁺ doping concentration. The efficient non-radiative energy

transfer processes between Dy3+ and Tb3+ allow a moderate concentration level of Tb3+ to achieve favorably

stronger spectral absorption at blue and ultraviolet wavelengths but almost negligible up-conversion.

Tb³⁺/Dy³⁺ co-doped phosphate glass shows promising potential for phosphors and lasing operation at

visible wavelengths.

Keywords: Dy³⁺/Tb³⁺; phosphate glass; luminescence; energy transfer process

* Corresponding author.

E-mail address: yufei@siom.ac.cn (F. Yu), hulili@siom.ac.cn (L. Hu)

1

1. Introduction

In recent years, visible luminescence of Tb³⁺ ions doped in crystal, ceramic and glass, has found various applications in display techniques, visible light communication and medical treatment ¹⁻⁶. Particularly, lasing operation in the visible spectral region has already been demonstrated in Tb³⁺ doped crystals, e.g. CaF₂⁷, LiLuF₄⁷, LiYF₄⁸, LaF₃⁹, KY₃F₁₀⁹, BaY₂F₈⁹, BaLu₂F₄⁹ as well as in fluoride glass fibers ¹⁰⁻¹².

Tb³⁺ doped fluoride glass was investigated for visible luminescence since 1989 13. Generally, the low-energy phonon density distribution of the fluoride glass mitigates the cross relaxation processes, which is favorable for a high concentration of rare-earth ions, and makes it an attractive material for gain fiber ¹⁰⁻¹², ¹⁴. In 2007, Tb³⁺ doped fluoride glass of 1 wt% concentration realized a gain of 5.3 dB at 540 nm wavelength ¹¹. In 2008, the first continuous-wave laser operation at 542 nm in a fluoride glass fiber was reported where 1.6 mW output power with 8.4 % slope efficiency was measured ¹².

Visible emissions in rare-earth ions doped oxide glasses usually suffer from degradation of emission strength due to the cross relaxation effect 15. Uniquely, Tb3+ ions with 5D4-multiplet are regarded as a promising doping candidate which is assumed to be largely absent from cross relaxation processes due to the lack of acceptor levels. The feasibility of doping Tb3+ ion in phosphate 16, silicate 17, and borate ¹⁸ glasses has been explored. Unfortunately the weak absorption cross section of Tb³⁺ around 10⁻²² cm² in the blue spectral region ⁹ challenges its practical application.

Among oxide glasses, phosphate glasses are known for high transparency, high solubility of rare-earth ions, low photo-darkening and mature manufacturing technology ¹⁹⁻²¹. Although in principle phosphate glasses allow a much higher doping concentration of Tb³⁺, multi-photon absorption ⁹ counterbalances the benefits of increased dopant concentration in practice. To address the dilemma, Dy³⁺ assisted energy transfer (ET) process has been proposed to enhance the visible fluorescence of Tb³⁺ under a moderate

concentration level and investigated in hosts of borate ²², silicate ²³ oxyfluorosilicate ²⁴ glasses, which indicated Dy³⁺ ion as a good sensitizer for the visible emission of Tb3+ ions.

In the previous studies of Dy3+/Tb3+ co-doped phosphate glasses 25-27, the potential of using Dy3+ to sensitize Tb3+ in phosphate glass for visible lasing application still remained unexplored. In this work, we focus on the spectroscopic properties of Tb3+ ions in Dy3+/Tb3+ co-doped phosphate glasses, and systematically characterize the dependence of spectral and temporal properties of Tb³+ emission on pump wavelength and Dy³+ concentration, which are key to understand the sensitization effect of Dy³+ ions. Energy transfer routes and corresponding efficiencies between Dy³+ and Tb³+ ions are investigated based on experimental measurement of enhanced absorption, excitation and fluorescence spectra of Tb³+ ions in the Dy³+/Tb³+ co-doped phosphate glass. We experimentally confirm much higher Judd–Ofelt parameters and longer lifetime of Tb³+ in our phosphate glass, with a promising potential for laser operation at visible wavelengths.

2. Glass synthesis and characterization methodology

2.1 Glass synthesis

The sample glasses are fabricated by composition (in mol%) of 65P₂O₅-15Al₂O₃-10K₂O-(10-x-y)Y₂O₃-xTb₂O₃-yDy2O3 (x=1, y=0, 0.1, 0.5, 1, 2; x=0, y=1; x=0, 0.5, 1, 2, 4, y=0.5) which are denoted as T1, T1D0.1, T1D0.5, T1D1 and T1D2, respectively), as listed in Table 1. Analytical reagents P₂O₅, Al₂O₃, K₂CO₃ and high purity Tb₂O₃, Dy₂O₃ (99.99 wt.% Aladdin Chemical Co.) were used as raw materials. Compounds were well mixed and melted in platinum crucibles at 1150°C for 2 h in the atmosphere, cast onto a preheated steel plate, and then annealed at 450°C for 3 h. The prepared glass samples (15 mm × 15 mm × 1.2 mm each) were double-polished for characterization.

Table 1. Composition of Tb3+/Dy3+ coped phosphate glasses.

Glass compositions (mol%)

Samples	P ₂ O ₅	Al ₂ O ₃	K ₂ O	Y ₂ O ₃	Tb ₂ O ₃	Dy ₂ O ₃
T1	65	15	10	9	1	-
T1D0.1	65	15	10	8.9	1	0.1
T1D0.5	65	15	10	8.5	1	0.5
T1D1	65	15	10	8	1	1
T1D2	65	15	10	7	1	2
D1	65	15	10	9	-	1
D0.5	65	15	10	9.5	-	0.5
T0.5D0.5	65	15	10	9	0.5	0.5
T2D0.5	65	15	10	7.5	2	0.5
T4D0.5	65	15	10	5.5	4	0.5

2.2 Measurement method

Phases of the samples were characterized by X-ray diffraction (XRD, Rigaku RINT-2000) with Cu Kα radiation (0.154 nm). The element distribution of samples was characterized by JXA8230 electron probe microscopy analysis (EPMA). Scanning electron microscopy (SEM) images of samples were acquired on an SU1080 microscopy (Hitachi, Japan). The refractive index was measured by a waveguide prism coupling instrument 1010/M (Metricon Co., USA). The absorption spectra of Dy³+/Tb³+ co-doped phosphate glass samples were measured with a UV/VIS/NIR spectrophotometer (Perkin Elmer Lambda 900) using Xe discharged lamp as light source. The excitation, emission spectra and fluorescence lifetime of samples were obtained by using an Edinburg FL920-type spectrophotometer. All measurements were carried out at room temperature.

3. Characterization and discussion

3.1 Dopant distribution in samples

The XRD patterns of all Dy³⁺/Tb³⁺ co-doped phosphate glasses are shown in Fig. 1, and a broad refraction peak at around $2\theta = 25^{\circ}$ was observed in all glass samples. Based on the study on the fundamentals of amorphous solids ²⁸, the broad refraction peak is ascribed to the immaterial orientation of the amorphous glass with regard to the X-ray beam as there is no any crystalline plane. The diffraction angle 2θ is related to the region of local random network in glasses (from Bragg's raw: $\lambda = 2d \sin \theta$). We pick T1D1 and

characterize 2D elemental distributions of P, O, Al and K shown in Fig. 2a–e, whereas the signals of low-concentrated Tb³⁺ and Dy³⁺ were too weak to detect. To further examine the dopant uniformity, we use EPMA to scan sample T1D2 and homogeneous distributions of Tb³⁺ and Dy³⁺ ions in Fig. 2f.

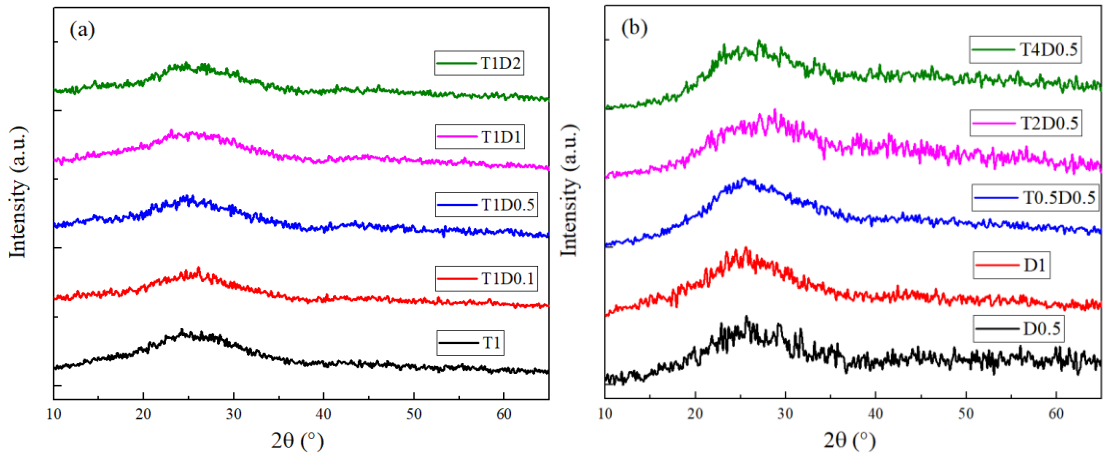


Fig. 1. XRD patterns of Tb³⁺/Dy³⁺ co-doped phosphate glasses.

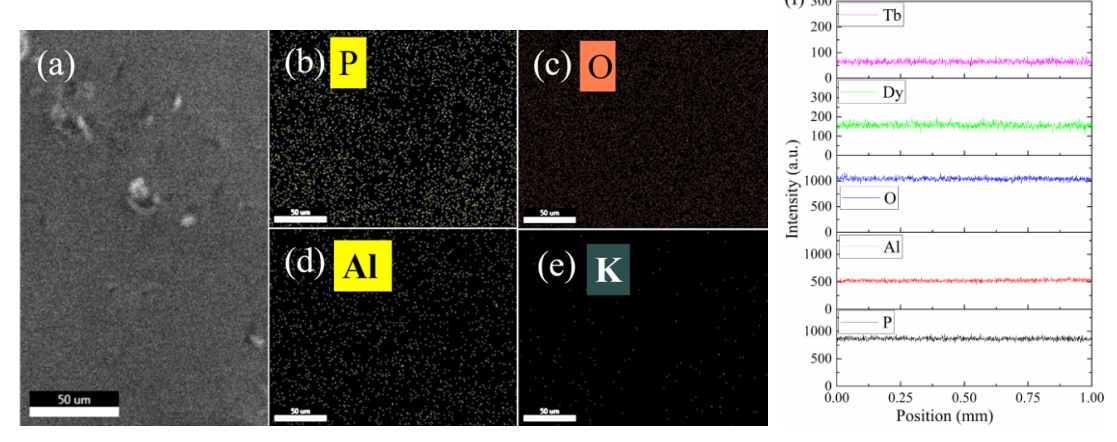


Fig. 2. (a) SEM images of glass surface and two-dimensional elemental distributions of (b) P, (c) O, (d) Al and (e) K in the T1D1 sample, and (f) line scan of P, Al, O, Dy and Tb in sample T1D2.

3.2 Absorption measurement and Judd-Ofelt analysis

The measured absorption spectra of all glass samples in the wavelength range from 300 to 2500 nm are shown in Fig. 3a and b. Absorption peaks of Tb³⁺ ions in Dy³⁺ free sample T1 locate at 338, 350, 359, 366, 377, 485, 1885, 1903 and 2209 nm corresponding to transitions from ground state ${}^{7}F_{6}$ to excited states of ${}^{5}L_{7}$, ${}^{5}L_{9}$, ${}^{5}G_{5}$, ${}^{5}L_{10}$, ${}^{5}D_{3}$, ${}^{5}D_{4}$, ${}^{7}F_{1}$, ${}^{7}F_{2}$ and ${}^{7}F_{3}$, respectively. Absorption in Dy³⁺/Tb³⁺ co-doped samples at 350, 364, 377, 386, 425, 452, 472 and 1682 nm is due to transitions of Dy³⁺ ions from ground state ${}^{6}H_{15/2}$ to the ${}^{4}M_{15/2}$, ${}^{4}I_{11/2}$, ${}^{4}I_{13/2}$, ${}^{4}F_{7/2}$, ${}^{4}G_{11/2}$, ${}^{4}I_{15/2}$, ${}^{4}F_{9/2}$ and ${}^{6}H_{11/2}$ excited states, as illustrated by the energy level diagrams

²⁵ in Fig. 3c. In the single dopant samples, Dy³⁺ ions present much stronger absorption than Tb³⁺ ions at the same concentration level at UV and blue wavelengths. By comparing Fig. 3a and b, Tb³⁺ ions show higher absorption at infrared wavelength region, whereas Dy³⁺ ions exhibit much stronger absorption at UV and blue wavelengths.

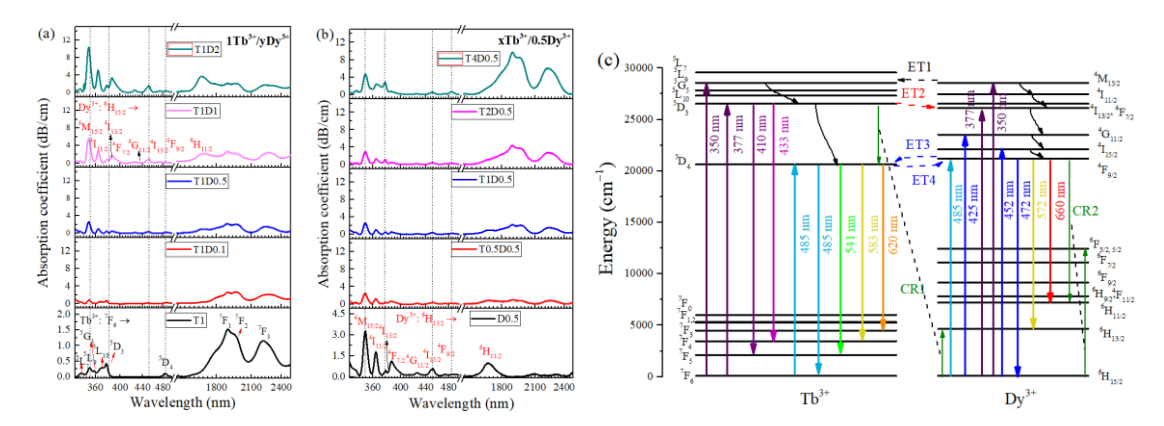


Fig. 3. Measured absorption spectra of (a) $1\text{Tb}^{3+}/\text{yDy}^{3+}$ (y=0, 0.1, 0.5, 1, 2), (b) $x\text{Tb}^{3+}/0.5\text{Dy}^{3+}$ (x=0, 0.5, 1, 2, 4) in phosphate glasses, and (c) energy level diagrams of Tb^{3+} and Dy^{3+} ions with possible transfer routes in between 25 .

Table 2. Absorption cross-sections σ_a of Tb³⁺ and Dy³⁺ ions at UV and visible wavelengths

Transitions	Wavelength (nm)	$\sigma_a(\times 10^{-22}\text{cm}^2)$ of Tb^{3+}	σ_{a} (×10 ⁻²² cm ²) of Dy ³⁺
Tb^{3+} : ${}^7F_6 \rightarrow {}^5L_9$	350	2.9	
$Tb^{3+}: {}^{7}F_{6} {\longrightarrow} {}^{5}D_{3}$	377	4.3	

$Tb^{3+}: {}^{7}F_{6} {\longrightarrow} {}^{5}D_{4}$	485	1.1	
Dy ³⁺ : ${}^{6}H_{15/2} \rightarrow {}^{4}M_{15/2}$	350		62.8
Dy ³⁺ : ${}^{6}H_{15/2} \rightarrow {}^{4}I_{11/2}$	364		35.1
Dy ³⁺ : ${}^{6}H_{15/2} \rightarrow {}^{4}I_{13/2}$	377		9.6
Dy ³⁺ : ${}^{6}H_{15/2} \rightarrow {}^{4}I_{15/2}$	452		8.9
Dy ³⁺ : ${}^{6}H_{15/2} \rightarrow {}^{4}F_{9/2}$	485		2.3

Based on Judd–Ofelt (J–O) theory 29,30 , the experimental strength (f_{exp}) of transitions can be calculated from absorption spectra by the following equation:

$$f_{\rm exp} = \frac{2.303mc^2}{\pi N l e^2 \overline{\lambda}^2} \int \log_{10} \left(\frac{I(\lambda)}{I_0} \right) d\lambda \tag{1}$$

where m is the electron mass, e the charge, c the velocity of light in vacuum, and $\bar{\lambda}$ the mean wavelength of the transition photon. The theoretical oscillator strength (f_{cal}) of radiative $4f \rightarrow 4f$ transitions from an initial J to a final J' states can be calculated:

$$f_{cal}(J;J') = \frac{8\pi^2 mc}{3h(2J+1)\bar{\lambda}} \left[\frac{(n^2+2)^2}{9n} S_{ed}(J;J') + nS_{md}(J;J') \right]$$
(2)

$$S_{ed}\left(J;J'\right) = \sum_{t=2,4,6} \Omega_{t} \left| \left\langle (S,L)J \left\| U^{t} \right\| (S',L')J' \right\rangle \right|^{2}$$
(3)

$$S_{md}(J,J') = \left(\frac{h}{4\pi mc}\right)^{2} \sum_{I=2,4,6} \left| \left\langle (S,L)J \| \bar{L} + 2\bar{S} \| (S',L')J' \right\rangle \right|^{2} \tag{4}$$

where n is the refractive index of the host, the terms $\left|\left\langle (S,L)J\right| |U^t| |(S',L')J'\right\rangle^2$ are the double-reduced matrix elements of unit tensor operators that are considered to be independent of host materials and its values of Tb³⁺ ions are given by Carnall et al. ³¹, and Ω_t (t=2, 4, 6) are the J–O parameters that can be calculated by a least-square fitting approach. Table 3 shows good agreement between $f_{\rm exp}$ and $f_{\rm eal}$. The root-mean-square deviation ($\delta_{\rm rms}$) is $\pm 0.12 \times 10^{-6}$ implying a good quality of fitting. It is noted that J–O parameters of Tb³⁺ ions in T1 sample are calculated from the absorption bands of $^7F_6 \rightarrow ^5D_4$ and $^7F_{1,2,3}$ (shown in Fig. 3a) rather than the absorption in the blue region (300–400 nm) where the absorption features are too complex to calculate 32,33 .

Table 3. Peak wavelength of absorption bands of Tb^{3+} ions in T1 sample as well as the experimental f_{exp} and calculated f_{cal} oscillator strengths.

Transition	$\lambda_{peak} (nm)$	$f_{\rm exp} (\times 10^{-6})$	$f_{\rm cal}$ (×10 ⁻⁶)
$^{7}\text{F}_{6} \rightarrow ^{5}\text{D}_{4}$	484	0.060	0.060
$^{7}\text{F}_{6} \rightarrow ^{7}\text{F}_{1}$	1895	0.585	0.495
$^{7}\text{F}_{6} \rightarrow ^{7}\text{F}_{2}$	1903	0.540	0.620
$^{7}\text{F}_{6} \rightarrow ^{7}\text{F}_{3}$	2209	0.645	0.629
		$\delta_{ m rms}$ $=$ ± 0 .	12×10^{-6}

Table 4 compares the J-O parameters of Tb³⁺ in our T1 sample with other reported host materials ^{18, 32-}

³⁵. The parameter Ω_2 reflects directly the asymmetry of local environment around Tb³⁺ ions and the covalence degree between Tb³⁺ and ligand ions. The spectroscopic quality factor Ω_4/Ω_6 is important for evaluating the stimulated emission behavior ³⁴. A higher values of Ω_2 parameter (21.60 × 10⁻²⁰ cm²) and Ω_4/Ω_6 ratio of 0.73 for Tb³⁺ ions are obtained in our phosphate glass (T1 sample) than those reported in previous studies, implying that a stronger local electric field results in a higher degree of asymmetry around the rare-earth ions and gives rise to a more efficient stimulated emission of Tb³⁺ ions in our phosphate glass.

Table 4. Comparison of Judd–Ofelt parameters of Tb³⁺ ions in different host materials.

Host materials	$\Omega_2 (10^{-20} \text{cm}^2)$	$\Omega_4 (10^{-20} \text{cm}^2)$	$\Omega_6 (10^{-20} \text{cm}^2)$	Ω_4/Ω_6	Reference
Lead borate glass	13.23	1.23	2.96	0.42	32
Lead telluroborate glass	11.98	2.87	10.51	0.27	33
Zinc borophosphate glass	11.26	1.02	3.00	0.34	34
Borate glass	6.95	1.28	2.91	0.44	18
Fluoride glass	13.40	2.15	4.90	0.44	35
Phosphate glass (T1)	21.60	1.56	2.15	0.73	Our work

3.3 Excitation and luminescence measurement

Figure 4 compares the measured excitation spectra of the T1 and T1D0.5 samples by monitoring the emission at 541 nm, as well as D1 sample monitored at 572 nm. According to Fig. 4, we select 350, 377 and 485 nm as pumping wavelengths, corresponding to Tb^{3+} : ${}^{7}F_{6} \rightarrow {}^{5}L_{9} + Dy^{3+}$: ${}^{6}H_{15/2} \rightarrow {}^{4}H_{15/2}$, Tb^{3+} : ${}^{7}F_{6} \rightarrow {}^{5}D_{3} + Dy^{3+}$: ${}^{6}H_{15/2} \rightarrow {}^{4}F_{7/2}$ and Tb^{3+} : ${}^{7}F_{6} \rightarrow {}^{5}D_{4} + Dy^{3+}$: ${}^{6}H_{15/2} \rightarrow {}^{4}F_{9/2}$, respectively, and investigate the fluorescence of Tb^{3+} ions as a function of Dy^{3+} concentration. The corresponding emission spectra are shown in Fig. 5.

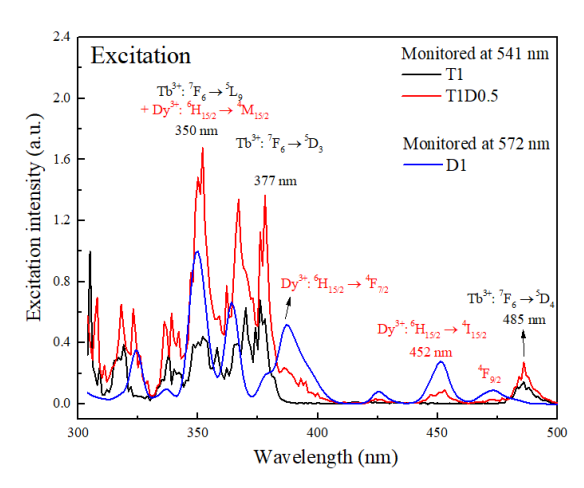


Fig. 4. Excitation spectra of the samples T1 and T1D0.5 by monitoring emission at 541 nm as well as D1 sample monitored at 572 nm.

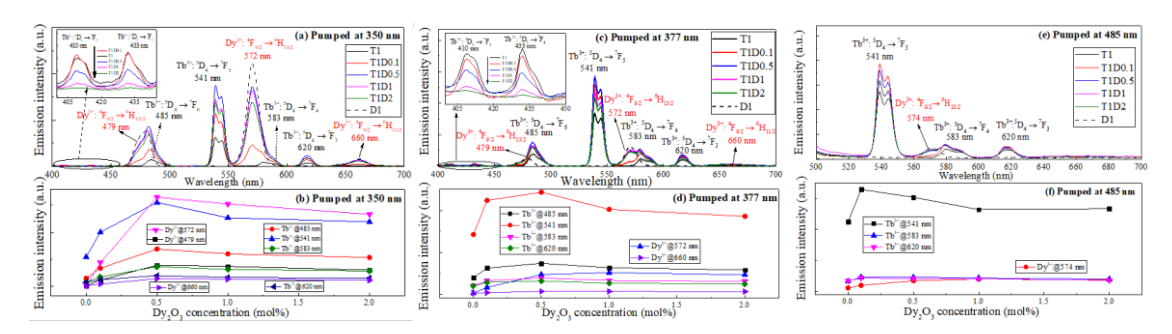


Fig. 5. Emission spectra of 1Tb³⁺/yDy³⁺ (y=0, 0.1, 0.5, 1, 2) co-doped phosphate glasses pumped by (a) 350 nm, (c) 377 nm and (e) 485 nm, and the corresponding trends of main emission intensities as a function of Dy³⁺ concentration pumped by (b) 350 nm, (d) 377 nm and (f) 485 nm, respectively.

In Fig. 5a, the emission of Tb³⁺ ions peaked at 541 nm is observed in T1 and much enhanced after introducing Dy³⁺ ions. By pumping at 350 nm wavelength, Tb³⁺ ions have a rapid thermal relaxation that would populate ⁵D₃ from ⁵L₉ ²⁵, and subsequently radiate to ⁷F₅ and ⁷F₄ states, giving rise to emission peaked at 412 and 435 nm, respectively (as shown in Fig. 3c). Meanwhile, electrons in ⁵D₃ state of Tb³⁺ would non-radiatively quench to ⁵D₄ state by multi-phonon relaxation or cross relaxation (CR) processes, and then radiate to ⁷F₆, ⁷F₅, ⁷F₄ and ⁷F₃ states corresponding the emissions peaked at 485, 541, 583 and 620 nm, respectively. Under pumping at 350 nm, Dy³⁺ ions are excited to ⁴M_{15/2} state and found quickly quenched to ⁴F_{9/2} state by thermal relaxation, and then radiate to ⁶H_{15/2}, ⁶H_{13/2} and ⁶H_{11/2} states which give rise to emissions at 479, 572 and 660 nm respectively. The introduction of Dy³⁺ ions helps population of Tb³⁺: ⁵D₃ state through the ET1 process (shown in Fig. 3c) efficiently. From the enhanced emission at 485, 541 and

620 nm wavelengths (derived from Tb^{3+} : 5D_4 state shown in Fig. 5a), we confirm a more efficient energy transfer process ET3 (shown in Fig. 3c) from Dy^{3+} ions to populate the Tb^{3+} : 5D_4 state. It is noted that the ET2 and CR1 (Tb^{3+} : ${}^5D_3 + Dy^{3+}$: ${}^6H_{15/2} \rightarrow Tb^{3+}$: ${}^5D_4 + Dy^{3+}$: ${}^6H_{13/2} + \text{phonon}$, shown in Fig. 3c) processes can reduce the emission strengths at 410 and 433 nm wavelengths, when Dy_2O_3 doping concentration is more than 0.5 mol%.

The emissions strength of Tb^{3+} reaches the maximum in all samples when introducing Dy^{3+} at 0.5 mol% Dy_2O_3 concentration. As the doping concentration of Dy^{3+} rises further, emission intensities of both Dy^{3+} and Tb^{3+} ions in T1D1 and 2 samples are declined and maintained, and we ascribe it to the counterbalance out of concentration quenching effect 36 , in which the ET4 process from Tb^{3+} to Dy^{3+} ions, and possible $CR2 (Dy^{3+}: {}^4F_{9/2} + {}^6H_{15/2} \longrightarrow {}^6H_{11/2} + {}^6F_{3/2}$ shown in Fig. 3c) occurred between Dy^{3+} ions 37 , resulted in the inefficient emission behaviors of Tb^{3+} and Dy^{3+} ions respectively.

Similar to 350 nm pumping wavelength, 377 nm pump will excite Tb³⁺: ⁵D₃ state, radiating to ⁷F₅ (412 nm) and ⁷F₄ (435 nm) states, meanwhile the ET2, ET3 and CR1 processes populate the Tb³⁺: ⁵D₄ state, radiating to ⁷F₆ (485 nm), ⁷F₅ (541 nm), ⁷F₄ (583 nm) and ⁷F₃ (620 nm) states. Emissions peaked at 485, 541, 583 and 620 nm show almost the same trends as that by pumping at 350 nm. For Dy³⁺ ions, a thermal relaxation will populate ⁴F_{9/2} from ⁴F_{7/2} (377 nm) states as shown in Fig. 3c, and generate 479, 572 and 660 nm emissions. The weak emissions of Dy³⁺ ions can be attributed to its lower absorption at 377 nm as shown in Table 1 and Fig. 4.

In Fig. 5e, the main emission at 541 nm is generated by pumping Tb^{3+}/Dy^{3+} co-doped phosphate glasses with 485 nm. The Tb^{3+} : 5D_4 state is populated by 485 nm pump and ET3 process from Dy^{3+} ions, radiating to 7F_6 (485 nm), 7F_5 (541 nm), 7F_4 (583 nm) and 7F_3 (620 nm) states. The maximum emission of Tb^{3+} appears in the T1D0.1 sample and the concentration quenching effect takes place for Dy_2O_3 concentration more

than 0.5 mol%, which are attributed to the lower absorption cross-sections of both Tb^{3+} and Dy^{3+} ions at 485 nm. It can be concluded for Dy^{3+} ions that all the pumping wavelengths (350, 377 and 485 nm) populate the Dy^{3+} : ${}^4F_{9/2}$ state, and generate emissions peaked at 479, 572 and 660 nm. Besides, 350 nm is the most efficient pump wavelength for both the 541 nm emission of Tb^{3+} and 572 nm emission of Dy^{3+} ions in Tb^{3+}/Dy^{3+} co-doped phosphate glasses.

3.4 Florescence lifetimes of Tb³⁺ ion

The fluorescence decay curve of Tb^{3+} : ${}^5D_4 \rightarrow {}^7F_5$ transition emitting at around 541 nm are measured as a function of Dy^{3+} concentrations under excitations of 350, 485 and 452 nm respectively, shown in Fig. 6. Using a logarithmic scale for the axis of emission intensity we confirm an almost linear fluorescence decay as function of time, indicating an expononential decay behavior. As shown in Fig. 6d, the longest lifetime of Tb^{3+} : 5D_4 state is found in T1D0.1 with 0.1 mol% Dy_2O_3 concentration for all pump wavelengths, which we ascribed to the ET3 process, whereas the slightly decreased lifetime 38 is attributed to the ET4 and CR2 processes shown in Fig. 3c. The trends of lifetime of Tb^{3+} : 5D_4 level as function of Dy^{3+} concentration almost show no dependence on pumping wavelengths as illustrated in Fig. 6d.

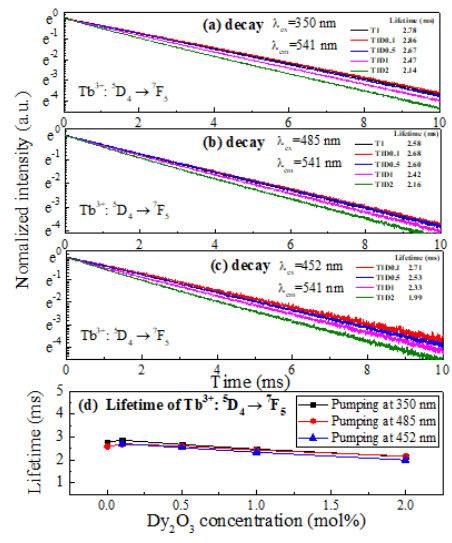


Fig. 6. Decay curves of transition Tb^{3+} : ${}^5D_4 \rightarrow {}^7F_5$ pumped at (a) 350 nm, (b) 485 nm and (c) 452 nm, and (d) the calculated lifetime as a function of Dy^{3+} concentration.

Table 5. Measured lifetime of the Tb^{3+} : ${}^5D_4 \rightarrow {}^7F_5$ transition in our work (pumped by 350 nm) and

reported literatures.

Host	Tb ₂ O ₃ concentration (mol%)	Lifetime (ms)	Reference
Lead borate glass	1.0	1.76	32
Lead telluroborate glass	1.0	0.83	33
Zinc borophosphate glass	0.9	1.89	34
Fluoride glass	0.5	1.21	35
T1	1.0	2.78	Our work
T1D0.1	1.0	2.86	Our work
T1D0.5	1.0	2.67	Our work
T1D1	1.0	2.47	Our work
T1D2	1.0	2.14	Our work

Table 5 compares the measured lifetime of Tb³⁺: ${}^5D_4 \rightarrow {}^7F_5$ transition in various host materials ${}^{32\text{-}35}$. The longest 2.86 ms lifetime of Tb³⁺: 5D_4 is measured in T1D0.1 sample.

3.5 Energy transfer efficiency and mechanism

The results of Fig. 4–6 show how the concentration of Dy^{3+} ions affect the visible emission properties and fluorescence lifetime of Tb^{3+} under the excitation of different pumping wavelength. To further investigate the energy transfer efficiency from Dy^{3+} to Tb^{3+} ions, we focus on the emission and fluorescence lifetime of $xTb^{3+}/0.5Dy^{3+}$ (x=0, 0.5, 1, 2, 4) co-doped glass samples by pumping at 425 nm where Tb^{3+} presents no absorption.

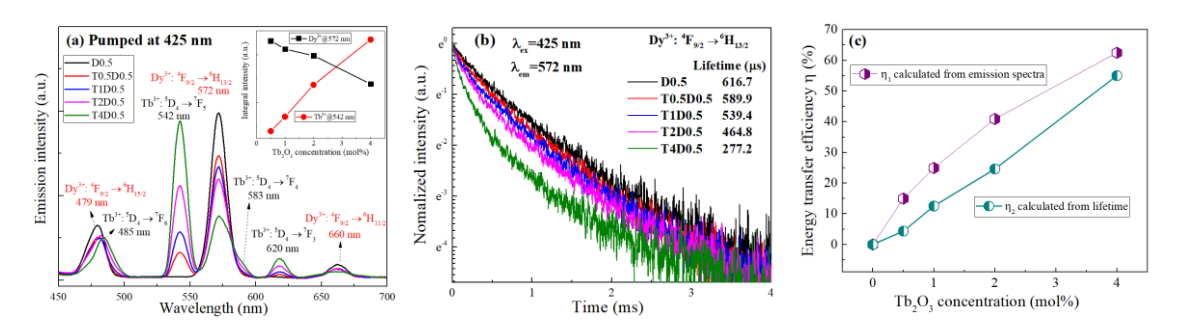


Fig. 7. (a) Emission spectra of $xTb^{3+}/0.5Dy^{3+}$ (x=0, 0.5, 1, 2, 4) co-doped phosphate glasses pumped by 425 nm, and the inset is the trends of main emission intensities, and (b) the decay curves of transition ${}^4F_{9/2} \rightarrow {}^6H_{13/2}$ of Dy^{3+} pumped by 425 nm, inset shows the energy transfer efficiency from Dy^{3+} to Tb^{3+} ions as a function of Tb^{3+} concentration.

Under excitation, Dy³⁺: ${}^4G_{11/2}$ state is populated and quickly relaxed by transferring energy to ${}^4F_{9/2}$ state, and radiate to ${}^6H_{15/2}$ (479 nm), ${}^6H_{13/2}$ (572 nm) and ${}^6H_{13/2}$ (660 nm) states as shown in Fig. 3c and Fig. 7a. Through ET3 process, Tb³⁺: 5D_4 state is excited with fluorescence emissions peaked at 541, 583 and 620

nm shown in Fig. 7a. After introducing Tb³⁺ ions, the energy transfer process ET3 populates the Tb³⁺: 5D_4 state and gives rise to an increased emissions strength of Tb³⁺ at all wavelengths when Tb³⁺ concentration rises. Based on the emission spectra, the energy transfer efficiency from Dy³⁺ to Tb³⁺ ions is defined by η_1 = $1-I_{Dy}/(I_{Dy}+I_{Tb})^{39}$, where I_{Dy} and I_{Tb} are the integrated intensities of Dy³⁺ and Tb³⁺ ions, respectively, and the calculated results are plotted in Fig. 7c. We obtained the increasing energy transfer efficiency from Dy³⁺ to Tb³⁺ ions as a function of Tb³⁺ concentration in our phosphate glasses, which are 15.0 %, 24.9 %, 40.9 % and 62.5 % for the T0.5D0.5, T1D0.5, T2D0.5 and T4D0.5 samples, respectively.

To complete our measurement, the decay curves of the transition Dy^{3+} : ${}^4F_{9/2} \rightarrow {}^6H_{13/2}$ (572 nm) under excitation at 425 nm are measured as a function of Tb^{3+} ions concentration shown in Fig. 7b. A non-exponential decay behavior of Dy^{3+} after introducing Tb^{3+} ions, especially in the T4D0.5 sample, which confirms the energy transfer processes between Dy^{3+} and Tb^{3+} ions. The average lifetimes are calculated by

$$\tau = \frac{\int_0^\infty t I(t)dt}{\int_0^\infty I(t)dt} \tag{5}$$

where I(t) is the emission intensity as function of time t. The lifetime of Dy³⁺ declined from 616.7 μ s (D0.5 sample) to 277.2 μ s (T4D0.5 sample) as listed in Table 6. Based on the fluorescence lifetime of Dy³⁺, the energy transfer efficiency from Dy³⁺ to Tb³⁺ ions can be also calculated by $^{25, 40, 41}$ η_2 =1 $-\tau/\tau_0$, in which τ_0 and τ represent lifetime of donor in the absence and presence of acceptor, respectively) and the calculated results are plotted in Fig. 7c, which are 4.4 %, 12.5 %, 24.6 % and 55.0 % as a function of Tb³⁺ concentration for the T0.5D0.5, T1D0.5, T2D0.5 and T4D0.5 samples, respectively. Both η_1 and η_2 values show a similar increasing trend as function of Tb³⁺ ions and the results in our phosphate glasses are on the same level as those found in other host materials $^{25, 40}$, indicating an efficient sensitizer of Dy³⁺ ion for the visible emission

of Tb³⁺ ions in our phosphate glasses.

Based on Dexter's energy transfer expressions of multipolar interactions ⁴² and Reisfeld's approximation ⁴³, the donor-acceptor energy transfer probability (P_{DA}) is defined as $P_{DA} = (1/\tau_d)(\eta_0/\eta_0-1)$, in which τ_d is lifetime of donor, η_0 and η are the luminescence quantum efficiencies of donor in the absence and presence of acceptor. The η_0/η can be approximately calculated by^{25, 41, 43}

$$\frac{\eta_0}{\eta} \approx \frac{I_0}{I} \propto C^{\frac{n}{3}} \tag{6}$$

where I_0 and I are the emission intensities of Dy³⁺ (572 nm) in the absence and presence of Tb³⁺ ions, respectively, C is the total concentration of Dy³⁺ and Tb³⁺ ions, and n = 6, 8 and 10 responding to electric dipole-dipole, dipole-quadrupole and quadrupole-quadrupole interactions, respectively. By linear fitting the dependece of I_0/I on $C^{n/3}$ as shown in Fig. 8, we obtained a linear relationship with the optimum $R^2 = 99.98\%$ only when n = 6, which indicates a dominant electric dipole-dipole interaction mechanism responsible for the energy transfer from Dy³⁺ to Tb³⁺ ions in our phosphate glasses. Table 6 summarized the calculated results discussed above, and in conclusion we obtained an increasing η_T and P_{DA} from Dy³⁺ to Tb³⁺ ions as a function of Tb³⁺ concentration under excitation at 425 nm. The chromaticity coordinate of emissions in xTb³⁺/0.5Dy³⁺ (x=0, 0.5, 1, 2, 4) co-doped samples excited at 425 nm in CIE1931 diagram (Fig. 9a) present a yellow-to-green light shift when Tb³⁺ concentration rises, indicating a potential application of using our glasses for color adjustable phosphors. Furthermore, we irradiate our Tb³⁺/Dy³⁺ co-doped phosphate glass byusing a 450 nm multi-mode laser diode (pumping Dy³⁺) as shown in Fig. 9b, and obtained a total reflection of green light in the glass, demonstrating a promising potential of using our Tb²⁺/Dy³⁺ co-doped phosphate glass for lasing operation at visible wavelengths.

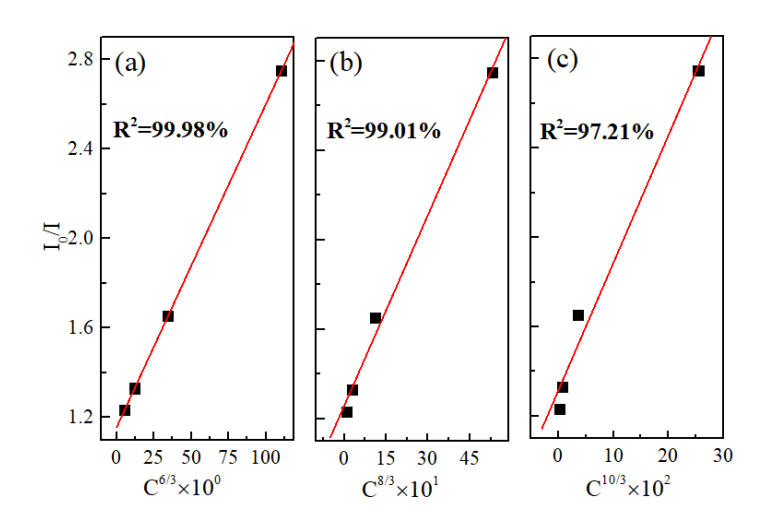
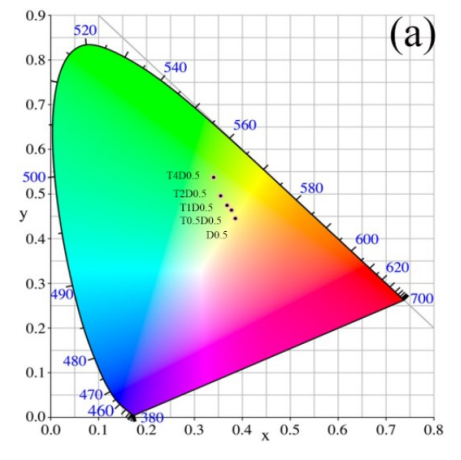


Fig. 8. Dependence of I_0/I on (a) $C^{6/3}$, (b) $C^{8/3}$ and (c) $C^{10/3}$.

Table 6. Measured lifetime τ of the Dy³⁺: ${}^4F_{9/2} \rightarrow {}^6H_{13/2}$ transition, energy transfer efficiencies η_T and probabilities (P_{DA}) as a function of Tb³⁺ concentration under excitation at 425 nm.

Samples	τ (μs)	η2 (%)	I_0/I	$P_{\mathrm{DA}}\left(\mathrm{s}^{-1}\right)$
D0.5	616.7			
T0.5D0.5	589.9	4.4	1.23	580.9
T1D0.5	539.4	12.5	1.33	874.1
T2D0.5	464.8	24.6	1.65	1405.2
T4D0.5	277.2	55.0	2.75	5795.3



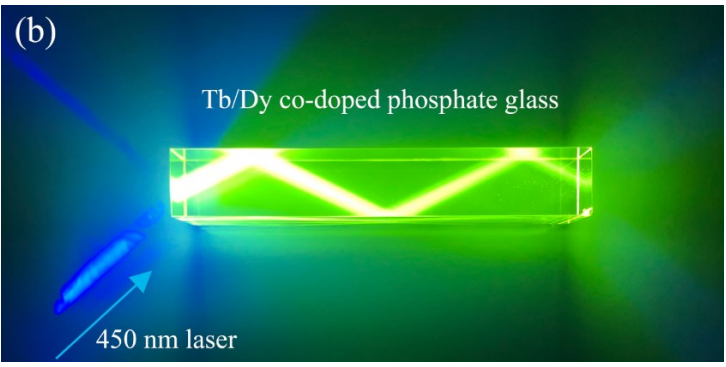


Fig. 9. (a) Chromaticity coordinates of emissions of $xTb^{3+}/0.5Dy^{3+}$ (x=0, 0.5, 1, 2, 4) co-doped samples

excited at 425 nm in CIE1931 diagram (b) photograph of Tb³⁺/Dy³⁺ co-doped phosphate glass under irradiation of 450 nm laser diode.

4. Conclusions

In this paper, we study the role of sensitization of Dy^{3+} ions played in the enhanced visible emission of Tb^{3+} ions in phosphate glasses at various pump wavelengths. We confirm that in the host of phosphate glass, the Judd–Ofelt parameters Ω_2 and Ω_4/Ω_6 for Tb^{3+} ions could reach up to 21.60×10^{-20} cm² and 0.73 respectively, highest among all glass hosts as far as we learn. The visible emission (peaked at 485 and 541nm) of Tb^{3+} ions can be much enhanced by the sensitization effect of Dy^{3+} under the excitation of 350 and 377 nm with an optimum Dy^{3+}/Tb^{3+} ions concentration ratio of 0.5:1. The maximum lifetime of $Tb^{3+}: {}^5D_4$ (2.86 ms) is measured for the concentration of Dy_2O_3 around 0.1 mol%. The energy transfer efficiency η_T from Dy^{3+} to Tb^{3+} is demonstrate an electric dipole-dipole interaction between them and also found a maximum η_T of 55.0% for 4:0.5 ratio of Tb^{3+}/Dy^{3+} at 425 nm wavelength for pumping. Our studies demonstrate a promising potential of Dy^{3+}/Tb^{3+} co-doped phosphate glasses for highly efficient visible phosphors and lasing applications.

Acknowledgements

This work was supported by National Key R&D Program of China (2018YFB0504500); Key Program for International S&T Cooperation Projects of China (2018YFE0115600); National Natural Science Foundation of China (NSFC, 51972317, 61875052, 61705244 and 61307056); National Natural Science Foundation, International (Regional) Cooperation and Exchange Program (61961136003). Natural Science Foundation of Shanghai (17ZR1433900, 17ZR1434200 and 18ZR1444400). Yu acknowledges the support of Chinese Academy of Sciences (CAS) Pioneer Hundred Talents Program. Knight acknowledges support of Chinese Academy of Sciences Presidential International Fellowship Initiative Grant No. 2019DT0015.

References

- Nakanishi J, Yamada T, Fujimoto Y, Ishii O, Yamazaki M. High-power red laser oscillation of 311.4 mW in Pr³⁺-doped waterproof fluoro-aluminate glass fibre excited by GaN laser diode, Electron Lett. 2010; 46(46): 1285–1286
- 2. Park H-A, Lee YK, Im WB, Heo J, Chung WJ. Phosphor in glass with Eu³⁺ and Pr³⁺-doped silicate glasses for LED color conversion, Opt Mater. 2015; 41: 67–70
- 3. Jiang S, Guo C, Che K, Luo Z, Du T, Fu H, et al. Visible Raman and Brillouin lasers from a microresonator/ZBLAN-fiber hybrid system, Photonics Res. 2019; 7(5): 566–572
- 4. Zhan L, Cai W, Li N, Lu J, Cai Z, Luo Z, et al. Direct generation of an ultrafast vortex beam in a CVD-graphene-based passively mode-locked Pr:LiYF₄ visible laser, Photonics Res. 2019; 7(11): 1209–1213
- 5. Lam EW, Little TDC. Visible light positioning: moving from 2D planes to 3D spaces [Invited], Chin Opt Lett. 2019; 17(3): 030604
- 6. Fangchen H, Yingjun Z, Nan C, Junlin L, Jianyang S, Fengyi J, et al. Common-anode LED on a Si substrate for beyond 15 Gbit/s underwater visible light communication, Photonics Res. 2019; 7(9): 09001019
- 7. Metz PW, Marzahl D-T, Huber G, Kränkel C. Performance and wavelength tuning of green emitting terbium lasers, Opt Exp. 2017; 25(5): 5716–5724
- 8. Jenssen HP, Castleberry D, Gabbe D, Linz A. Stimulated emission at 5445 Å in Tb³⁺: YLF, IEEE J Quantum Elect. 1973; 9: 665–665
- 9. Metz PW, Marzahl D-T, Majid A, Kränkel C, Huber G. Efficient continuous wave laser operation of Tb³⁺-doped fluoride crystals in the green and yellow spectral regions, Laser Photonics Rev. 2016; 10(2): 335–344
- 10. Yamashita T, Ohishi Y. Amplification and lasing characteristics of Tb³⁺-doped fluoride fiber in the 0.54 μm band, Jpn J Appl Phys. 2007; 46(No. 41): L991–L993
- 11. Yamashita T, Ohishi Y. Optical amplification at 0.54 μm by Tb³⁺-doped fluoride fibre, Electron Lett. 2007; 43(2): 88–90
- 12. Yamashita T, Qin G, Suzuki T, Ohishi Y, A new green fiber laser using terbium-doped fluoride fiber, in Optical Fiber Communication Conference/National Fiber Optic Engineers Conference. *OSA Technical Digest (CD)*. p. JWA18.
- 13. Amaranath G, Buddhudu S, Bryant FJ. Emission properties of Tb³⁺-doped alkali mixed fluoride glasses, Solid State Commun. 1989; 72(9): 923–925
- 14. Smart RG, Hanna DC, Tropper AC, Davey ST, Carter SF, Szebesta D. CW upconversion lasing at blue, green and red wavelengths in an infrared-pumped Pr³⁺-doped fluoride fibre at room temperature, Electron Lett. 1991; 27(14): 1307–1309
- 15. Zhang L, Xia Y, Shen X, Wei W. Concentration dependence of visible luminescence from Pr³⁺-doped phosphate glasses, Spectrochim Acta A. 2019; 206: 454–459
- 16. Zhang L, Peng M, Dong G, Qiu J. An investigation of the optical properties of Tb³⁺-doped phosphate glasses for green fiber laser, Opt. Mater. 2012; 34(7): 1202–1207
- 17. Baccaro S, Dall'Igna R, Fabeni P, Martini M, Mares JA, Meinardi F, et al. Ce³⁺ or Tb³⁺-doped phosphate and silicate scintillating glasses, J Lumin. 2000; 87–89: 673-675
- 18. Takebe H, Nageno Y, Morinaga K. Compositional dependence of Judd–Ofelt parameters in silicate, borate, and phosphate glasses, J Am Ceram Soc. 1995; 78(5): 1161–1168
- 19. Pugliese D, Boetti NG, Lousteau J, Ceci-Ginistrelli E, Bertone E, Geobaldo F, et al. Concentration quenching in an Er-doped phosphate glass for compact optical lasers and amplifiers, J Alloy Compd. 2016;

- 657: 678-683
- 20. Hu L, He D, Chen H, Wang X, Meng T, Wen L, et al. Research and development of neodymium phosphate laser glass for high power laser application, Opt Mater. 2017; 63: 213–220
- 21. Guo J, Wang J, Wei H, Huang W, Huang T, Xia G, et al. High-power, Joule-class, temporally shaped multipass ring laser amplifier with two Nd:glass laser heads, High Power Laser Sci Eng. 2019; 7: e8
- 22. Lin H, Pun EY-B, Wang X, Liu X. Intense visible fluorescence and energy transfer in Dy³⁺, Tb³⁺, Sm³⁺ and Eu³⁺ doped rare-earth borate glasses, J Alloy Compd. 2005; 390(1): 197–201
- 23. Sun X-Y, Gu M, Huang S-M, Liu X-L, Liu B, Ni C. Enhancement of Tb³⁺ emission by non-radiative energy transfer from Dy³⁺ in silicate glass, Physica B. 2009; 404(1): 111–114
- 24. Ramachari D, Moorthy LR, Jayasankar CK. Energy transfer and photoluminescence properties of Dy³⁺/Tb³⁺ co-doped oxyfluorosilicate glass–ceramics for solid-state white lighting, Ceram Int. 2014; 40(7, Part B): 11115–11121
- 25. Caldiño U, Muñoz H G, Camarillo I, Speghini A, Bettinelli M. Down-shifting by energy transfer in Tb³⁺/Dy³⁺ co-doped zinc phosphate glasses, J Lumin. 2015; 161: 142–146
- 26. Sobha KC, Rao KJ. Luminescence of, and energy transfer between Dy³⁺ and Tb³⁺ in NASICON-type phosphate glasses, J. Phys. Chem. Solids. 1996; 57(9): 1263–1267
- 27. Juárez-Batalla J, Meza-Rocha AN, Muñoz H G, Caldiño U. Green to white tunable light emitting phosphors: Dy³⁺/Tb³⁺ in zinc phosphate glasses, Opt. Mater. 2017; 64: 33–39
- 28. Stachurski ZH, Fundamentals of amorphous solids: structure and properties. Wiley-VCH, Higher Education Press, 2015.
- 29. Ofelt GS. Intensities of crystal spectra of rare-earth ions, J Chem Phys. 1962; 37(3): 511–520
- 30. Judd BR. Optical absorption intensities of rare-earth ions, Phys Rev. 1962; 127(3): 750-761
- 31. Carnall WT, Fields PR, Rajnak KJ. Electronic energy levels of the trivalent lanthanide aquo ions. III. Tb³⁺, J Chem Phys. 1968; 49(10): 4447–4449
- 32. Jamalaiah BC, Suresh Kumar J, Mohan Babu A, Sasikala T, Rama Moorthy L. Study on spectroscopic and fluorescence properties of Tb³⁺-doped LBTAF glasses, Physica B. 2009; 404(14): 2020–2024
- 33. Jamalaiah BC, Vijaya Kumar MV, Rama Gopal K. Investigation on luminescence and energy transfer in Tb³⁺-doped lead telluroborate glasses, Physica B. 2011; 406(14): 2871–2875
- 34. Bindu SH, Raju DS, Krishna VV, Raju CL, Preparation and characterization of Tb³⁺ ions doped zincborophosphate glasses for green emission, in AIP Conference Proceedings. Vol. 1849. p. 020002.
- 35. Amaranath G, Buddhudu S, Bryant FJ. Spectroscopic properties of Tb³⁺-doped fluoride glasses, J Non-Cryst Solids. 1990; 122(1): 66–73
- 36. Dornauf H, Heber J. Concentration-dependent fluorescence-quenching in La_{1-x}Pr_xP₅O₁₄, J. Lumin. 1980; 22(1): 1–16
- 37. Reddy Prasad V, Babu S, Ratnakaram YC. Concentration dependent luminescence properties of Dy³+doped lead free zinc phosphate glasses for visible applications, Indian J. Phys. 2016; 90(10): 1173–1182
- 38. M.Vijayakumar, K.Viswanathan, K.Marimuthu. Structural and optical studies on Dy³⁺:Tb³⁺ co-doped zinc leadfluoro-borophosphate glasses for white light applications, J Alloy Compd. 2018; 745: 306–318
- 39. Velázquez JJ, Rodríguez VD, Yanes AC, delCastillo J, MéndezRamos J. Increase in the Tb³⁺ green emission in SiO₂-LaF₃ nano-glass-ceramics by codoping with Dy³⁺ ions, J Appl Phys. 2010; 108(11): 628
- 40. Zur L, Kos A, Górny A, Sołtys M, Pietrasik E, Pisarska J, et al. Influence of acceptor concentration on crystallization behavior and luminescence properties of lead borate glasses co-doped with Dy³⁺ and Tb³⁺ ions, J Alloy Compd. 2018; 749: 561-566

- 41. Sun XY, Yu XG, Jiang DG, Wang WF, Li YN, Chen ZQ, et al. Spectroscopic and energy transfer properties of Dy³+-doped, Tb³+/Dy³+-codoped dense oxyfluoride borogermanate scintillating glasses, J Appl Phys. 2016; 119(23): 233103.233101-233103.233108
- 42. Dexter DL. A theory of sensitized luminescence in solids, J Chem Phys. 1953; 21(5): 836-850
- 43. Reisfeld R, Greenberg E, Velapoldi R, Barnett B. Luminescence quantum efficiency of Gd and Tb in borate glasses and the mechanism of energy transfer between them, J Chem Phys. 1972; 56(4): 1698-1705